Technical University of Denmark

DTU

Assembly of a novel biosynthetic pathway for production of the plant flavonoid fisetin in Escherichia coli

Stahlhut, Steen Gustav; Siedler, Solvej; Malla, Sailesh; Harrison, Scott James; Maury, Jerome; Neves, Ana Rute; Förster, Jochen

Published in:
Metabolic Engineering

Link back to DTU Orbit

DTU Library
Technical Information Center of Denmark

Assembly of a novel biosynthetic pathway for production of the plant flavonoid fisetin in *Escherichia coli*

Steen G. Stahlhut, Solvej Siedler, Sailesh Malla, Scott J. Harrison, Jérôme Maury, Ana Rute Neves, Jochen Forster *

Novo Nordisk Foundation Center for Biosustainability, Technical University of Denmark, Kogle Allé 6, 2970 Hørsholm, Denmark

A B S T R A C T

Plant secondary metabolites are an underutilized pool of bioactive molecules for applications in the food, pharma and nutritional industries. One such molecule is fisetin, which is present in many fruits and vegetables and has several potential health benefits, including anti-cancer, anti-viral and anti-aging activity. Moreover, fisetin has recently been shown to prevent Alzheimer's disease in mice and to prevent complications associated with diabetes type I. Thus far the biosynthetic pathway of fisetin in plants remains elusive. Here, we present the heterologous assembly of a novel fisetin pathway in *Escherichia coli*. We propose a novel biosynthetic pathway from the amino acid, tyrosine, utilizing nine heterologous enzymes. The pathway proceeds via the synthesis of two flavanones never produced in microorganisms before – garbanzol and resokaempferol. We show for the first time a functional biosynthetic pathway and establish *E. coli* as a microbial platform strain for the production of fisetin and related flavonols.

© 2015 International Metabolic Engineering Society Published by Elsevier Inc. On behalf of International Metabolic Engineering Society. This is an open access article under the CC BY-NC-ND license (http://creativecommons.org/licenses/by-nc-nd/4.0/).

1. Introduction

Flavonoids are ubiquitous polyphenolic secondary metabolites produced in many plants. Based on molecular structure, they can be subdivided into flavonols, flavones, flavonones, isoflavones, catechins, and anthocyanins (Winkel-Shirley, 2001). They are an important potential source for bioactive molecules. Polyphenols have been shown to have anti-inflammatory, anti-oxidant, anti-viral, anti-bacterial, anti-cancer, anti-proliferative, and anti-arteriosclerotic activities (Clere et al., 2011; Gresele et al., 2011; Middleton et al., 2000; Pan et al., 2010; Ross and Kasum, 2002).

Today flavonoids are mainly obtained by extraction from plants. Generally, the efficient and cost effective production of flavonoid compounds continues to be a major challenge. Extraction from plant material can be unreliable due to unexpected seasonal changes that may affect plant availability, while the complexity of the flavonoids themselves limit de novo chemical synthesis of these compounds (Keasling, 2010; Matkowski, 2008; Paterson and Anderson, 2005). In addition, production by chemical synthesis or plant extraction coincides with the use of toxic chemicals and large amounts of extraction solvents.

The development of microbial cell factories through metabolic engineering of heterologous biosynthetic pathways into microbes has emerged as a promising cost effective and more environmentally friendly alternative for large-scale production of flavonoids. Many genes from plants, bacteria and fungi, have been cloned and expressed in both *Escherichia coli* and *Saccharomyces cerevisiae* for production of flavonoid compounds, such as naringenin, liquiritigenin, pinocembrin and resveratrol (Hwang et al., 2003; Katz et al., 2011; Leonard and Koffas, 2007; Wu et al., 2013; Yan et al., 2005; Yan et al., 2007). Furthermore, the microbial production of flavonoids has emerged as an excellent economical alternative with a production process characterized by simple, readily available, inexpensive starting materials as well as the potential for lower waste emission and energy requirements (Chemler et al., 2006; Katsuyama et al., 2008; Keasling, 2010).

One of the flavonoids presently receiving increased attention is fisetin, a bioactive flavonol molecule found in many fruits and vegetables such as strawberry, apple, persimmon, grape, onion, and cucumber at concentrations ranging from 2 to 160 µg/g (Khan et al., 2012). Fisetin has been reported to display anti-aging (Maher, 2009), anti-inflammatory (Cho, et al., 2012; Kim et al., 2012), anti-carcinogenic (Ying et al., 2012) and anti-viral (Kang et al., 2012; Zandi et al., 2011) properties. In addition, it is claimed to be an orally active neuroprotective and memory-enhancing molecule (Maher et al., 2006; Sagara et al., 2004). Recently, fisetin has been suggested as a new approach for the treatment of Alzheimer's

* Corresponding author.
  E-mail address: jfor@biosustain.dtu.dk (J. Forster).

disease by Currais et al. (2013) and has been shown to prevent complications associated with diabetes type I (Maher et al., 2011).

In plants, the aromatic amino acids, L-tyrosine and L-phenyla-lanine are the precursors of phenolic compounds, such as flavo-noids and stilbenes. In this study, we focus on L-tyrosine as a precursor for the production of *para* (*p*)-coumaric acid. This can subsequently be converted into *p*-coumaroyl-coenzyme A (CoA) by tyrosine ammonia-lyase (TAL) and 4-coumaroyl-CoA ligase (4CL), respectively (Fig. 1). The biosynthetic pathway can be directed either (1) to naringenin by chalcone synthase (CHS) that converts one molecule of *p*-coumaroyl-CoA and three molecules of malonyl-CoA into naringenin chalcone, which is then isomerized into naringenin by chalcone isomerase (CHI) or (2) to liquiritigenin by CHS and chalcone reductase (CHR) that converts one molecule of *p*-coumaroyl-CoA and three molecules of malonyl-CoA into isoliquiritigenin. Thus, produced isoliquiritigenin is isomerized into liquiritigenin in presence of CHI (Fig. 1). In plants, these flavanone molecules can serve as a common intermediate from which the biosynthetic pathway can diverge resulting in a panoply of flavonoids (not shown in Fig. 1). Among the multiple side branches one can produce fisetin in plants. However, the biosyn-thetic pathway of fisetin remains unknown. Here, we propose a novel biosynthetic pathway for the production of fisetin from L-tyrosine and report the production of fisetin in *E. coli*.

Based on the molecular structure of fisetin, we hypothesized that fisetin (as well as garbanzol and resokaempferol) could be synthesized via a similar pathway to the quercetin biosynthetic pathway (Fig. 1). Fisetin and quercetin have very similar struc-tures; in fact, hydroxylation of the 5 position in the A ring of fisetin yields quercetin. It is known that quercetin is biosynthesized from the (2S)-flavanone naringenin. Naringenin is converted into dihy-drokaempferol that is further converted into kaempferol using flavanone 3-hydroxylase (F3H) and flavonol synthase (FLS),

utilizing O_2 and α-ketoglutarate (a-KG). In the final step of the synthetic pathway, quercetin is synthesized from kaempferol. In plants, this flavonoid hydroxylation step is usually performed by cytochrome P450 flavonoid monooxygenase (FMO) associated to a cytochrome P450 reductase (CPR), utilizing O_2 and NADPH (Leonard et al., 2006). We hypothesized that fisetin could be synthesized from liquiritigenin (Fig. 1). *p*-Coumaroyl-CoA is con-verted into isoliquiritigenin by CHS and CHR. CHI converts iso-liquiritigenin into liquiritigenin, from here the biosynthetic pathway proceeds to garbanzol, a compound similar in structure to dihydrokaempferol however lacking the OH group on the A ring of the flavonone (Fig. 1). Furthermore, we hypothesized that resokaempferol could be an intermediate in the conversion of garbanzol to fisetin. Resokaempferol is structurally similar to kaempferol, which is found in the quercetin biosynthetic pathway, except for the hydroxyl OH group in the A ring of the flavonone (Fig. 1). Overall, we suggest that the production of fisetin could occur via a pathway analogous to the biosynthetic pathway leading to quercetin production. Thus, three steps catalyzed by F3H, FLS and FMO/CPR utilizing O_2, NADPH and a-KG as cofactors would convert liquiritigenin to fisetin through the intermediates garbanzol and resokaempferol (Fig. 1).

2. Materials and methods

2.1. Bacterial strains and plasmids

All strains, vectors, and plasmids used in this study are listed in Table 1. *E. coli* DH5α (Invitrogen) was used for plasmid cloning and propagation, while *E. coli* BL21(DE3) was used for flavonoid production. Vectors pACYCDuet-1, pETDuet-1, pCDFDuet-1 and pRSFDuet-1 (Novagen) were used for cloning and subcloning.
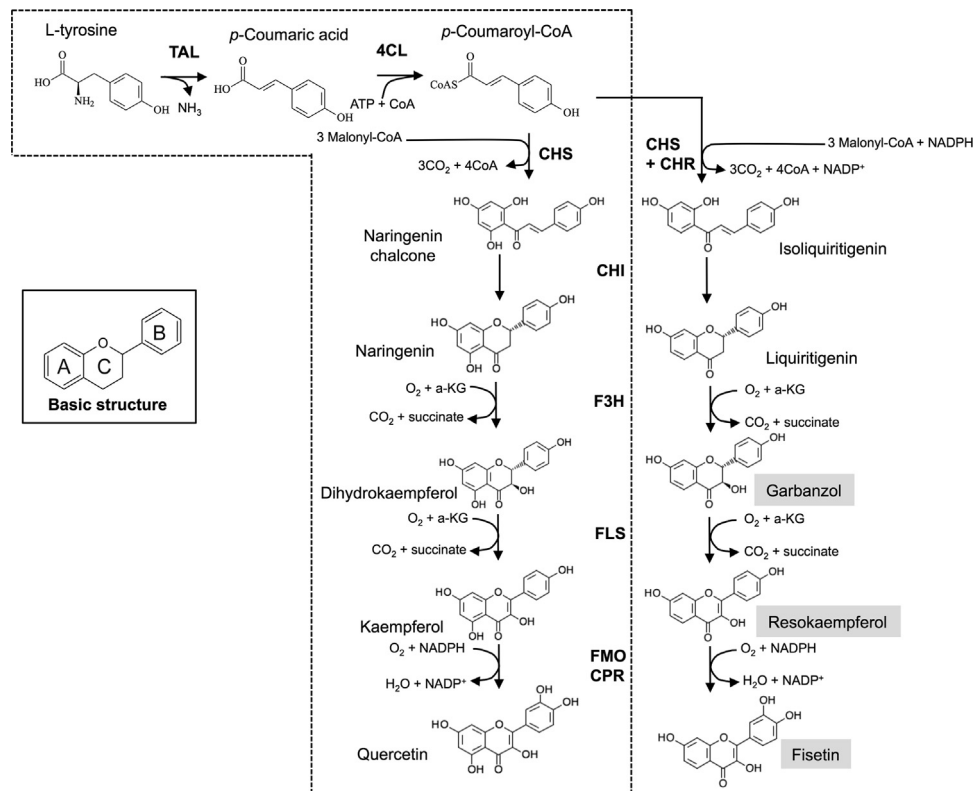
Fig. 1. Plant specific phenylpropanoid pathway for the synthesis of the flavonoid quercetin (inside dotted line) and proposed phenylpropanoid pathway for the synthesis of the flavonoid fisetin (outside the dotted line). TAL, tyrosine ammonia-lyase; 4CL, 4-coumaroyl-CoA lyase; CHS, chalcone synthase; CHR, chalcone reductase; CHI, chalcone isomerase; F3H, flavanone 3-hydroxylase; FLS, flavonol synthase; FMO, flavonoid 3′-monooxygenase; CPR and cytochrome P450 reductase.

Table 1
Bacterial strains and plasmids used in the study.

Strain/plasmid	Description	Reference
E. coli strains		
DH5α	General cloning host	Invitrogen
BL21(DE3)	*ompT hsdT hsdS* (r_B^- m_B^-) *gal* (DE3)	Novagen
ST1	BL21(DE3) carrying pCDF-*talRs-4cl-2Pc* and pET-*chsPh-chiMs*	This Study
ST2am	BL21(DE3) carrying pCDF-*talRs-4cl-2Pc* and pET-*chsPh-chiMs* and pRSF-*chrAm*	This Study
ST2fusion	BL21(DE3) carrying pRSF-*talRs-4cl-2Pc* and pET-*chsPhchrAm-chiMs*	This Study
ST3	BL21(DE3) carrying pCDF-*f3hAt-fls-1At*	Malla, 2013
ST4at	BL21(DE3) carrying pACYC *f3′hAt-cprCr*	This Study
ST4fxa1	BL21(DE3) carrying pACYC *f3′hFxa1-cprCr*	This Study
ST4fxa2	BL21(DE3) carrying pACYC *f3′hFxa2-cprCr*	This Study
ST4ph	BL21(DE3) carrying pACYC *f3′hPh-cprCr*	This Study
ST4mxd	BL21(DE3) carrying pACYC *f3′hMxd-cprCr*	This Study
ST4cr	BL21(DE3) carrying pACYC *f3′5′hCr-cprCr*	Leonard, 2006
ST5at	BL21(DE3) carrying pRSF-*talRs-4cl-2Pc* and pET-*chsPhchrAm-chiMs* pCDF-*f3hAt-fls-1At* and pACYC *f3′hAt-cprCr*	This Study
ST5ph	BL21(DE3) carrying pRSF-*talRs-4cl-2Pc* and pET-*chsPhchrAm-chiMs* pCDF-*f3hAt-fls-1At* and pACYC *f3′hPh-cprCr*	This Study
Plasmid vectors		
pETDuet-1	Double T7 promoters; ColE1 ori Amp^r	Novagen
pCDFDuet-1	Double T7 promoters; CloDF13 ori Sm^r	Novagen
pACYCDuet-1	Double T7 promoters; P15A ori Cm^r	Novagen
pRSFDuet-1	Double T7 promoters; RSF ori Km^r	Novagen
pCDF-*4cl-2Pc*	pCDFDuet-1 carrying *4cl*-2 from *P. crispum*	Leonard, 2006
pET-*chsPh-chiMs*	pETDuet-1 carrying *chs* from *P. hybrida* and *chi* from *M. sativa*	Leonard, 2007
pCDF-*talRs-4cl-2Pc*	pCDF-*4cl-2Pc* carrying *tal*[a] from *R. sphaeroides*	This Study
pRSF-*talRs-4cl-2Pc*	pRSFDuet-1 carrying *tal*[a] from *R. sphaeroides* and *4cl*-2 from *P. crispum*	This Study
pET-*chsPhchrAm-chiMs*	pETDuet-1 carrying *chs* from *P. hybrida* fused with *chr*[a] from *A. mongholicus* and *chi* from *M. sativa*	This Study
pRSF-*chrAm*	pRSFDuet-1 carrying *chr*[a] from *A. mongholicus*	This Study
pCDF*f3hAt-fls-1At*	pCDFDuet-1 carrying *f3h* and *fls* from *A. thaliana*	Malla, 2013
pACYC*f3′hAt-cprCr*	pACYCDuet-1 carrying *f3′h*[a] from *A. thaliana* and *cpr* from *C. roseus*	This Study
pACYC*f3′hFxa1-cprCr*	pACYCDuet-1 carrying *f3′h*[a] from *F. x ananassa* (1) and *cpr* from *C. roseus*	This Study
pACYC*f3′hFxa2-cprCr*	pACYCDuet-1 carrying *f3′h*[a] from *F. x ananassa* (2) and *cpr* from *C. roseus*	This Study
pACYC*f3′hMxd-cprCr*	pACYCDuet-1 carrying *f3′h*[a] from *M. x domestica* and *cpr* from *C. roseus*	This Study
pACYC*f3′5′hCr-cprCr*	pACYCDuet-1 carrying *f3′h*[a] from and *cpr* from *C. roseus*	Leonard, 2006
pACYC*f3′hPh-cprCr*	pACYCDuet-1 carrying *f3′h*[a] from *P. hybrida* and *cpr* from *C. roseus*	This Study

[a] Denotes that genes have been codon optimized for *E. coli*.

Plasmids pCDF-*4cl-2Pc* (Leonard, et al., 2006), pET-*chsPh-chiMs* (Leonard and Koffas, 2007) and pCDF-*f3hAt-fls-1At* (Malla et al., 2013) were previously reported.

2.2. Culture media and chemicals

E. coli was grown in 2 × yeast extract and tryptone (2 × YT) broth or on Luria–Bertania (LB) agar plates supplemented with the appropriate amount of antibiotics (100 µg ml^{-1} ampicillin, 25 µg ml^{-1} chloramphenicol, 50 µg ml^{-1} streptomycin/spectinomycin, and 35 µg ml^{-1} kanamycin), when necessary, for the selection or maintenance of the plasmids. M9 minimal media with 0.2% (w/v) glucose were used throughout for flavonoid production. In addition, 2% (w/v) glycerol was added to the M9 minimal media for the evaluation of fisetin production from ʟ-tyrosine.

Authentic standards of *p*-coumaric acid, naringenin, isoliquiritigenin, kaempferol, dihydrokaempferol, quercetin, quercetin-3-O-glucoside and fisetin were purchased from Sigma-Aldrich Co. (Denmark). Furthermore, authentic standards of naringenin chalcone, liquiritigenin and resokaempferol were acquired from Micro-CombiChem e.K. (Germany), Tocris Bioscience (United Kingdom) and Extrasynthese (France), respectively.

2.3. DNA manipulations

Recombinant DNA techniques were performed according to standard procedures (Sambrook et al., 1989). Restriction enzymes and T4 DNA ligase were purchased from Thermo scientific, Fermentas. Moreover, Gibson assembly master mix were purchased from New England Biolabs and utilized according to the manufacturer's instructions.

PCR was carried out using phusion polymerase from New England Biolabs. Oligonucleotide primers were purchased from Integrated DNA Technologies, BVBA (Belgium). All PCR primers used in this study are described in Supplementary Table 1.

Codon optimized genes for *E. coli* were purchased from GeneArt® (Life Technologies™).

2.4. Plasmid construction

For a detailed description of plasmid construction see Supplementary materials and methods.

2.5. Recombinant protein expression and flavonoid production and extraction

Unless otherwise stated flavonoid production was carried out as follows, *E. coli* BL21(DE3) harboring recombinant plasmids was precultured in 3 ml of 2 × YT liquid medium with appropriate antibiotics and incubated at 37 °C and 250 rpm overnight. The following day, the preculture was transferred into 2 ml of M9 minimal media (0.2% glucose), with appropriate antibiotics, to a final concentration of OD$_{600}$ 0.05 and cultured at 37 °C and 300 rpm in 24 deep well plates (Enzyscreen B.V., Netherlands) until OD$_{600}$ reached ~0.6. Then, Isopropyl β-ᴅ-1 thiogalactopyranoside (IPTG) was added at a final concentration of 1 mM, the cells grown for 3 h (h) at 30 °C, followed by addition of substrate. The cultures were cultured using an Innova® 44 orbital shaken with a 5 cm swing (New Brunswick Scientific). Depending on the experiment, either final concentrations of 0.5 mM ʟ-tyrosine, 0.075 mM purified resokaempferol, 0.1 mM liquiritigenin or 0.05 mM liquiritigenin was added and the culture was incubated

at 30 °C for 24 h. In the case of fisetin production from reso-kaempferol, samples were collected at 3 h, 24 h and 48 h, after addition of resokaempferol. For fisetin production from L-tyrosine samples were collected at 48 h, after addition of L-tyrosine. For production of liquiritigenin, collected samples were harvested by centrifugation at 13,000 rpm (16,200g) for 10 min and the super-natant was filtered through 0.2 μm filters and analysed by high-performance liquid chromatography (HPLC). Garbanzol, reso-kaempferol and fisetin were extracted directly from 750 μl culture by adding an equal volume of 99% ethanol (EtOH) followed by vigorous shaking for one hour. After centrifugation at 13,000 rpm (16,200g) for 10 min the supernatant was collected and filtered through 0.2 μm filters and injected into the HPLC. Experiments were carried out in triplicates. Sample preparation for HPLC of garbanzol and resokeampferol production, BL21(DE3) harboring pCDF-f3hAt-fls-1At was precultured as described above. The fol-lowing day, the preculture was transferred into 20 ml of M9 minimal medium with antibiotics, to a final concentration of OD$_{600}$ 0.05 and cultured at 37 °C and 300 rpm until OD$_{600}$ of ~0.6 was reached. Then IPTG was added to a final concentration of 1 mM and the culture was incubated for 5 h to increase biomass. The cell pellet was collected by centrifugation and resuspended in 100 ml of M9 minimal media supplemented with 1 mM of IPTG and 0.1 mM liquiritigenin and cultured at 30 °C and 300 rpm. The extraction was carried out as previously described by Malla et al. (2013). Briefly, the culture was extracted with an equal volume of ethyl acetate and organic layer was collected followed by evapora-tion of excess solvent to dryness. The remaining products were dissolved in 99% EtOH for HPLC fractionation, as well as mass spectrometry (MS) analysis for compound identification.

Stability assays of flavonoid compounds are described in Supplementary materials and methods.

2.6. Flavonoid analysis and quantification

The production of flavonoids in recombinant *E. coli* strains were analysed and quantified using a Dionex Ultimate 3000 HPLC with a Discovery® HS F5-5 column (4.6 by 150 mm; 5.0-μm particle size; Sigma-Aldrich) connected to a UV detector (277, 290, 333 and 370 nm). Depending on the flavonoid analysed two different methods were utilized. (A) A flow rate of 1.5 ml/min was used with a linear gradient of 10 mM ammonium formate pH 3.0 buffer (mobile phase A) and acetonitrile (mobile phase B) by the following method: 0–0.5 min (5% B), 0.5–7 min (5 to 60% B), 7–9.5 min (60% B), 9.5–9.6 min (60 to 5% B), and 9.6–12 min (5% B). Under these conditions, L-tyrosine was detected at 2.5 min (277 nm), p-coumaric acid at 5.6 min (333 nm), liquiritigenin at 6.8 min (277 nm), nar-ingenin at 7.5 min (290 nm) and isoliquiritigenin at 8.0 min (370 nm) of retention times, respectively. Authentic L-tyrosine, p-coumaric acid, liquiritigenin, naringenin and isoliquiritigenin were used as standards. Calibration curves of authentic p-coumaric acid, naringenin, liquiritigenin and isoliquiritigenin were used for quantification. (B) A flow rate of 1 ml/min was used with a linear gradient of 10 mM ammonium formate pH 3.0 buffer (mobile phase A) and acetonitrile (mobile phase B) by the following method: 0–2 min (20% B), 2–20 min (20–45% B), 20–22 min (45–20% B), and 22–24 min (20% B). Under these conditions, dihydrokaempferol was detected at 10.0 min (333 nm), fisetin at 10.3 min (370 nm), liquir-itigenin at 12.8 min (277 nm), resokaempferol at 13.3 min (3 7 0), quercetin at 13.9 min (370 nm), naringenin at 16.7 min (290 nm), kaempferol at 17.2 min (370 nm) and isoliquiritigenin 19.9 min (370 nm) of retention times, respectively. Authentic dihydrokaemp-ferol, fisetin, liquiritigenin, resokaempferol, quercetin, naringenin, kaempferol and isoliquiritigenin were used as standards. Calibration curves of authentic resokaempferol and authentic fisetin were used for quantification. Putative garbanzol and resokaempferol peaks

were purified using a semi prep a Dionex Ultimate 3000 HPLC equipped with a fraction collector, using a Discovery® HS F5-5 column (4.6 by 150 mm; 5.0-μm particle size; Sigma-Aldrich) connected to a UV detector (277, 290, 333 and 370 nm). A flow rate of 1 ml/min was used with a linear gradient of 10 mM ammonium formate pH 3.0 buffer (mobile phase A) and acetonitrile (mobile phase B) by the following method: 0–3 min (20% B), 3–21 min (20–45% B), 21 to 23 min (45%B), 23 to 25 min (45–20% B) and 25–33 min (20% B).

2.7. Elucidation of garbanzol, resokaempferol and fisetin

The previously isolated compounds (garbanzol and resokaemp-ferol) were dried at room temperature under reduced pressure using a Centrifugal Vacuum Concentrator (Savant SpeedVac® Concentrator, Thermofisher Scientific, Waltham Ma) followed by reconstitution using a 0.1% solution of formic acid in LC-MS grade acetonitrile (250 μl). The samples (produced fisetin, garbanzol and resokaempferol) were then analysed by directed infusion on a VelosPro linear ion trap mass spectrometer (Thermofisher Scien-tific, Waltham Ma), using the built-in syringe pump, (set at a flow rate of 10 μl min^{-1}). Both positive and negative ion electrospray modes were used, with data being collected in centroid mode. MS^1 and MS^2 spectra for each sample were acquired; the MS^2 were acquired at collision energies of 30 V and 40 V in both ionization modes.

3. Results

3.1. Production of liquiritigenin from L-tyrosine

To verify the upstream part of the proposed pathway, we initially obtained pCDF-4cl-2Pc – the pCDFDuet-1 plasmid carrying the native 4cl-2 gene from *Petroselinum crispum* as well as pET-chsPh-chiMs – the pETDuet-1 plasmid carrying the native chs from *P. hybrida* and the native chi gene from *Medicago Sativa* (Leonard et al., 2006; Leonard and Koffas, 2007). TAL from *R. sphaeroides* (TALrs), codon optimized for *E. coli*, was cloned into the pCDF-4cl-2Pc recombinant plasmid, upstream of the 4cl-2 gene, under the T7 promoter in MCS1 (4CLpc is located downstream of the T7 promoter in MCS2). Subse-quently, the talrs4clpc DNA fragment was subcloned into the pRSFDuet-1 vector. pRSF-talRs-4cl-2Pc and pET-chsPh-chiMs were then transformed into BL21(DE3) creating *E. coli* strain ST1 synthe-sizing naringenin (Table 2). Production of liquiritigenin requires the expression of CHR, the branch point enzyme, in addition to CHS. Therefore, pRSF-chrAm was constructed, using a codon optimized chr gene from *A. mongholicus* (CHRam) followed by transformation into *E. coli* BL21(DE3) strain ST1 creating strain ST2am. CHR from *A. mongholicus* has recently been characterized (Xu et al., 2012). Hypothesizing that CHS co-act with CHR in catalyzing the substrate p-coumaroyl-CoA into isoliquiritigenin, the two genes were fused together, only separated by a linker consisting of glycine and serine creating pET-chsPhchrAm-chiMs. Together with pRSF-talRs-4cl-2Pc this fusion plasmid was transformed into *E. coli* BL21(DE3), resulting in strain ST2fusion. As expected, when supplemented with 0.5 mM L-tyrosine, strains ST1, ST2am and ST2fusion all produced naringenin, while only ST2am and ST2fusion produced isoliquiritigenin and liquiritigenin (Table 2). Interestingly, when CHS and CHR were fused together the production of liquiritigenin was increased by almost four-fold (Table 2). An *E. coli* strain carrying both of the empty vectors pRSFDuet-1 and pETDuet-1 did not produce naringenin, liquiriti-genin or isoliquiritigenin.

Table 2
The production of *p*-coumaric acid (PCA), naringenin (NRN), liquiritigenin (LIQ) and isoliquiritigenin (ILQ) using recombinant *E. coli* strains ST2am, ST2fusion and ST1.

	Production (mg l−1)			
	PCA	NRN	LIQ	ILQ
ST2am	17.6 ± 0.25	0.22 ± 0.03	0.51 ± 0.08	0.13 ± 0.02
ST2fusion	13.0 ± 2.31	0.11 ± 0.01	1.84 ± 0.23	0.41 ± 0.07
ST1	10.2 ± 0.39	0.81 ± 0.08	0 ± 0.0	0 ± 0.0

3.2. Production of garbanzol and resokaempferol

In order to confirm the assumption that F3H and FLS are active on liquiritigenin through the intermediates garbanzol and reso-kaempferol, native F3H and FLS from *Arabidopsis thaliana* were utilized by transforming plasmid pCDF-*f3hAt-fls-1At* into BL21 (DE3) creating *E. coli* strain ST3. F3H and FLS have previously been shown to convert naringenin into dihydrokaempferol and kaempferol, respectively by introducing a hydroxyl group in the C-3 position of the C ring followed by the formation of a double bond between the C-2 and C-3 carbons in the C ring of the chalcone structure (Fig. 1, synthesis of flavonol from dihydroflavonol) (Malla et al., 2012; Malla et al., 2013; Leonard et al., 2006). F3H and FLS were selected based on the high structural similarities between dihydrokaempferol and garbanzol as well as kaempferol and resokaempferol (Fig. 1).

ST3 was cultivated and production of dihydrokaempferol and kaempferol was detected after 24 h upon supplying the cells with naringenin (Fig. 2A, B).

The flavonoids were identified by HPLC comparing the retention times and UV absorbance spectra of the extracted flavonoids with authentic compounds. F3H and FLS from *A. thaliana* showed activity towards naringenin, producing dihydrokaempferol and kaempferol. No dihydrokaempferol or kaempferol were detected in a control experiment using BL21(DE3) carrying pCDFDuet-1 (Fig. 2C).

Subsequently, *E. coli* strain ST3 was evaluated for production of garbanzol and resokaempferol after 24 h upon supplementing the cells with liquiritigenin (Fig. 2D). The identification of garbanzol is putative as no authentic garbanzol is commercially available or could be obtained to be used as a standard compound. Liquiritigenin was detected after a retention time of 12.8 min and isoliquiritigenin after a retention time of 19.9 min. Resokaempferol was detected at a retention time of 13.3, confirmed by UV spectra and retention time comparison with an authentic resokaempferol standard. An unknown peak in the chromatogram at 8.0 min was observed (Figure D). Since naringenin and dihydrokaempferol displayed similar UV spectra's, it was hypothesized that the unidentified peak could be garbanzol (Fig. 2) based on the high similarities observed for the UV spectra between liquiritigenin and putative garbanzol (Fig. 2E). No peaks similar to putative garbanzol and resokaempferol were detected in a control experiment using BL21(DE3) carrying pCDFDuet-1 (Fig. 2E). Isoliquiritigenin was detected in the control experiment, as liquiritigenin can be non-enzymatically isomerized into isoliquiritigenin at both high and neutral pH conditions, and at temperatures above 4 °C (Simmler et al., 2013). The UV-spectra of all the compounds are shown in Fig. 2.

3.3. Elucidation of garbanzol and resokaempferol

To firmly assign the identity of the flavonoids produced in the engineered *E. coli* strain, ST3 was cultured in M9 minimal media (0.2% glucose) for 48 h upon supplementation with liquiritigenin. Flavonoid compounds were extracted with an equal volume of ethyl acetate and injected into an HPLC-fraction collector and the

peaks tentatively assigned as resokaempferol and garbanzol purified. After purification the putative garbanzol and resokaempferol were injected into a high resolution LC-MS (Thermo Orbitrap Fusion™) for further elucidation and compound identification with ms^n (Supplementary Fig. 1A and B). The spectra for the compound tentatively assigned as garbanzol showed an ion with m/z 273.07565 which corresponds to within −0.4 ppm of the mass of an ion with the ionic formula of $C_{15}H_{13}O_5$ in positive ion mode and an ion with m/z 271.06055 corresponds to within −2.4 ppm of the mass of an ion with the ionic formula of $C_{15}H_{11}O_5$ in negative ion mode, indicative of a compound with a molecular formula of $C_{15}H_{12}O_5$ (Supplementary Fig. 1A). This finding is consistent with the isolated molecule being garbanzol having a molecular formula of $C_{15}H_{12}O_5$. Furthermore, infusion of the purified resokaempferol gave a spectra (Supplementary Fig. 1B), which showed an ion with m/z 271.06005 corresponding to within −0.2 ppm of an ion with the ionic formula of $C_{15}H_{11}O_5$ in positive ion mode and an ion with m/z 269.04521 corresponding to within −1.3 ppm of an ion with the ionic formula of $C_{15}H_9O_5$ in negative ion mode. Infusion of the resokaempferol standard (Supplementary Fig. 1C) gave ions with m/z 271.06010 corresponding to within 0.0 ppm of an ion with the ionic formula of $C_{15}H_{11}O_5$ in positive ion mode and m/z 269.04521 corresponding to within −1.4 ppm of an ion with the ionic formula of $C_{15}H_9O_5$ in negative ion mode. Examination of the MS^2 spectra revealed that the fragmentation patterns are consistent with each other.

3.4. Cytochrome P450 screening and fisetin production

In order to elucidate the final step in the putative fisetin biosynthetic pathway, from resokaempferol to fisetin, a set of different cytochrome P450 monooxygenases (F3′H, flavonoid 3′ monooxygenase) were evaluated. The genes were selected based on (i) novelty (ii) likelihood of participation in fisetin production in strawberry as well as (iii) previous characterizations (Thill et al., 2013; Leonard et al., 2006). To examine the functional expression of the genes, a previously described method was utilized, with minor modifications (Leonard et al., 2006, Hotze et al., 1995). Initially, all of the genes were codon optimized for *E. coli*, truncated, fused with truncated cytochrome P450 reductase (CPR, codon optimized) from *C. roseus*, cloned into pACYCDuet-1 and transformed into BL21 (DE3), respectively. Thus, the following strains were created: ST4at carrying F3′H from *A. thaliana*; ST4fxa1 and ST4fxa2 carrying F3′Hs from two subspecies of *F. x ananassa*, ST4mxd carrying F3′H from *M. x domestica* and ST4ph carrying F3′H from *P. hybrida*. Furthermore, a previously described strain, that had been shown to convert kaempferol into quercetin, ST4cr carrying F3′5′H from *C. roseus* (Leonard et al., 2006) was reconstructed in a similar manner as described above. However, unlike in the previous study, the gene was codon optimized for *E. coli*. In order to evaluate the six strains, 0.05 mM resokaempferol was supplied, and bioconversion products were analysed after 3 h, 18 h and 40 h of cultivation, by HPLC, comparing the retention times and UV absorbance spectra of flavonoids with authentic fisetin and authentic resokaempferol (Fig. 3). Three hours after addition of resokaempferol, five strains: ST4cr, ST4at, ST4fxa2, ST4mxd and ST4ph produced fisetin in detectable amounts. The highest amount was observed from ST4at at 1.2 mg l^{-1} of fisetin, followed by ST4ph producing 0.25 mg l^{-1}, ST4fxa2 producing 0.15 mg l^{-1} and ST4cr and ST4mxd both producing 0.04 mg l^{-1} of fisetin (Fig. 3). ST4fxa1 and BL21(DE3) containing an empty pACYCDuet-1 vector did not produce any fisetin after 3 h. At 18 h after addition of resokaempferol, fisetin was detected in samples from ST4at at 2.1 mg l^{-1}, ST4ph at 0.92 mg l^{-1}, ST4fxa2 at 0.1 mg l^{-1} and ST4cr at 0.6 mg l^{-1}. For ST4fxa1, ST4mxd and BL21 (DE3) containing an empty pACYCDuet-1 vector, fisetin was not detected. After 40 h, fisetin was detected in amounts varying from
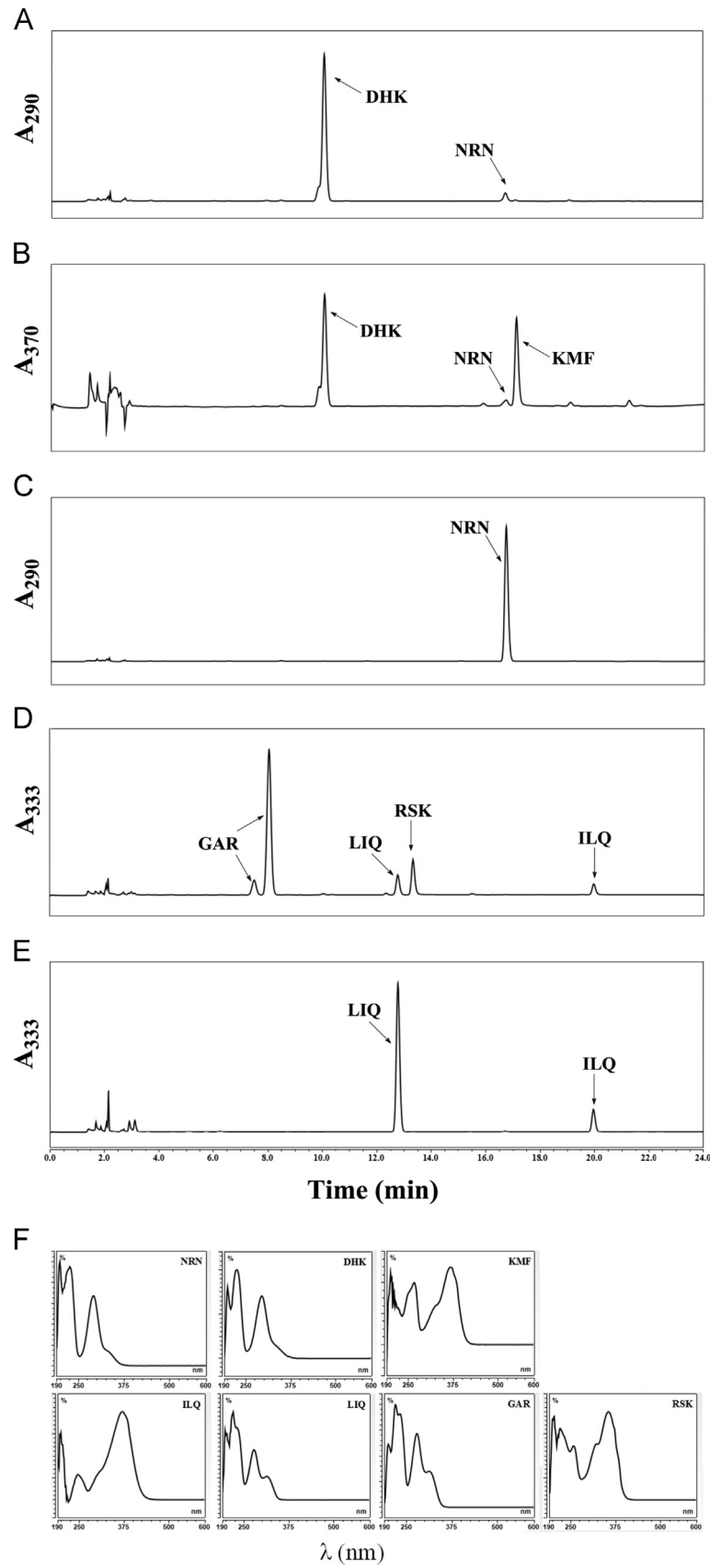
Fig. 2. Typical HPLC profile of (A) naringenin supplemented *E. coli* strain ST3 at wavelength 290 nm (B) naringenin supplemented *E. coli* strain ST3 at wavelength 370 nm (C) naringenin supplemented *E. coli* strain carrying pCDFDuet-1 at wavelength 290 nm (D) liquiritigenin supplemented *E. coli* strain ST3 at wavelength 333 nm (E) liquiritigenin supplemented *E. coli* strain carrying pCDFDuet-1 at wavelength 333 nm. (F) UV spectra of HPLC analysed compounds. NRN denotes naringenin, DHK – dihydrokaempferol, KMF – kaempferol, ILQ – isoliquiritigenin, LIQ – liquiritigenin, GAR – garbanzol and RSK – resokaempferol. Experiments were carried out in triplicates.
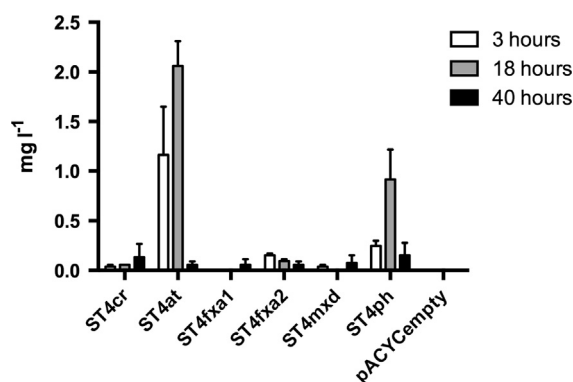
Fig. 3. Resokaempferol supplemented *E. coli* strains carrying truncated codon optimized CPR from *C. roseus* and codon optimized F3′H from *A. thaliana* (ST4at), *F. x ananassa* 1 (ST4fxa1), *F. x ananassa* 2 (ST4fxa2), *P. hybrida* (ST4ph) and *M. X domestica* (ST4mxd) as well as F3′5′H from *C. roseus* (ST4cr). Concentration (mg l^{-1}) of fisetin in samples after 3 h (white bars), 18 h (gray bars) and 40 h (black bars) after addition of resokaempferol are displayed. Experiments were carried out in triplicates. The mean values of three experiments are shown along with SEM.

0.06 to 0.15 mg l^{-1} in all of the strains expressing P450 monooxygenase. For BL21(DE3) containing an empty pACYCDuet-1 vector, fisetin was not detected after 40 h. The decrease of the fisetin concentration over time suggests that fisetin is unstable in M9 minimal media (see below).

Overall, the P450s evaluated here from various origins, all showed conversion of resokaempferol to fisetin. Subsequently, in order to verify that we indeed produce fisetin, a collected sample from ST4cr was evaluated further. The HPLC detected peak which eluted at the same retention time as the fisetin standard was analysed on a linear ion trap and therefore the masses are reported at unit mass (Supplementary Fig. 2A). The observed ions 287 in positive mode and 285 are consistent with those observed in the fisetin standard. The spectra for the infusion of the fisetin standard (Supplementary Fig. 2B) gave an ion with *m/z* 287.05487 which corresponds to within −0.5 ppm of ion with the ionic formula of $C_{15}H_{11}O_6$ in positive ion mode and an ion with *m/z* 285.03997 corresponds to within −1.7 ppm of ion with the ionic formula of $C_{15}H_9O_6$ in positive ion mode, indicative of compound with a molecular formula of $C_{15}H_{10}O_6$. The MS^2 spectra show that the fragmentation patterns in both positive and negative ionization modes are consistent with both spectra being from fisetin.

3.5. Fisetin production from L-tyrosine

To investigate the complete biosynthetic pathway from L-tyrosine to fisetin, pRSF-*talRs-4cl-2Pc* pET-*chsPhchrAm-chiMs* and pCDF-*f3hAt-fls-1At* was transformed into ST4at, and ST4ph, respectively, creating ST5at and ST5ph. The two constructed strains were cultivated (0.5 mM of L-tyrosine was supplied), and bioconversion products were analysed after 48 h of cultivation by HPLC analysis, comparing the retention times and UV absorbance spectra of flavonoids with authentic fisetin as well as all of the intermediates in the pathway (Table 3).

E. coli strain ST5at was cultured in M9 minimal media containing 0.2% (w/v) glucose. However, only *p*-coumaric acid and garbanzol could be detected (data not shown). Subsequently, in order to increase the biomass *E. coli* strains ST5at and ST5ph were cultured in M9 minimal media containing 0.2% (w/v) glucose and 2% (w/v) glycerol. Remarkably, in addition to *p*-coumaric acid and garbanzol both ST5at and ST5ph produced fisetin (Table 3). Thus, after 48 h of cultivation ST5at produced 10.0 mg l^{-1} of *p*-coumaric acid, a detectable amount of garbanzol (no standard could be obtained for quantification) and 0.25 mg l^{-1} of fisetin while ST5ph produced 12.1 mg l^{-1} of *p*-coumaric acid, a detectable amount of

Table 3
Production of fisetin (FIS) and detected intermediates, *p*-coumaric acid (PCA) and garbanzol (GAR) from L-tyrosine using recombinant *E. coli* strains ST5at and ST5ph.

	Production (mg l-1)	
	ST5at	**ST5ph**
PCA	10.0 ± 1.0	12.1 ± 4.29
GAR	Detected	Detected
FIS	0.25 ± 0.04	0.3 ± 0.12
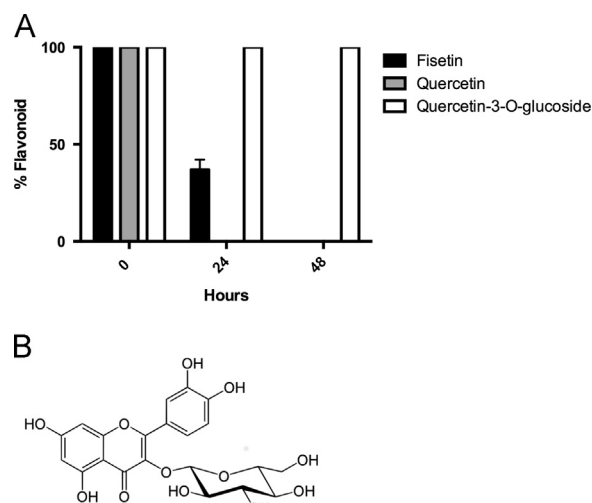
Fig. 4. (A) Stability of fisetin, quercetin and quercetin-3-O-glucoside in M9 minimal media at 30 °C at time 0 h, 24 h and 48 h. Experiments were carried out in triplicates. The mean values of three experiments are shown along with SEM. (B) quercetin-3-O-glucoside.

garbanzol and 0.3 mg l^{-1} of fisetin. The produced fisetin was successfully verified by high resolution LC-MS (Thermo Orbitrap Fusion™) (data not shown). No other intermediates of the pathway were detected. No compounds were detected in control samples containing *E. coli* strain BL21(DE3) carrying all four empty vectors, pCDFDuet-1, pRSFDuet-1, pETDuet-1 and pACYCDuet-1. Thus, the production of fisetin in bacteria is reported for the first time.

3.6. Stability of flavonoids

The instability of fisetin in M9 media prompted the investigation of the other compounds in the quercetin and fisetin pathways for stability issues. Therefore, L-tyrosine, *p*-coumaric acid, isoliquiritigenin, naringenin chalcone, liquiritigenin, naringenin, garbanzol, dihydrokaempferol, resokaempferol, kaempferol, quercetin and fisetin were evaluated for stability in M9 media over a period of 48 h without presence of *E. coli* in the media.

Non-enzymatically isomerization of isoliquiritigenin and liquiritigenin as well as of naringenin chalcone and naringenin was herein confirmed (data not shown) (Simmler et al., 2013). Dihydrokaempferol was not degraded after 24 h, however after 48 h dihydrokaempferol was not detected and naringenin appeared, suggesting a non-enzymatic dehydration of dihydrokaempferol to naringenin in M9 media (data not shown).

Intriguingly, apart from dihydrokaempferol, of the compounds evaluated here, only fisetin and quercetin showed instability in M9 media, suggesting that the flavonol molecule becomes instable with the addition of a second –OH group to the C-ring (of the basic structure) (Fig. 4A). To investigate if the stability of the flavonol molecule could be increased, quercetin-3-O-glucoside was

evaluated in the stability assay (Fig. 4A&B). Indeed, addition of a sugar molecule to quercetin (glycosylation) rendered the molecule stable (Fig. 4A).

4. Discussion

There is an increasing demand for a stable/sustainable supply of high quality and novel bioactive ingredients. Flavonoids represent a promising group of molecules that may find application as pharmaceutical drugs or nutraceutical ingredients. Here, a synthetic fisetin pathway comprised of genes from various heterologous sources (mostly plants) was assembled and the functional expression in *E. coli* verified.

In recent years, introduction and expression of natural plant pathways in non-native hosts such as *E. coli* and other microorganisms have proven to be a robust and sustainable alternative (Keasling, 2010). However, pathway elucidation and subsequently the validation thereof play an important role for the successful production of flavonoids in the selected heterologous host organism. Despite fisetin being found in various plants, its natural biosynthetic pathway has yet to be fully elucidated. Since fisetin is a valuable plant natural product from both a human health and economic perspective, the characterization of fisetin's biosynthetic pathway is pivotal in order to generate new approaches for its production.

At the onset of this work, we hypothesized a novel biosynthetic pathway for the production of fisetin from L-tyrosine, inspired by the biosynthetic pathway of quercetin.

The upstream part of the proposed pathway was evaluated by expressing TAL, 4CL, together with CHS, CHI and CHR in *E. coli*. Interestingly, accumulation of *p*-coumaric acid was detected independently of the expression of the CHR enzyme, in all three strains investigated here. This suggests that the 4CL from *P. crispum* is a limiting factor in the pathway. Furthermore, in the presence of *p*-coumaric acid, *E. coli* has been shown to up-regulate an efflux pump (Licandro-Seraut et al., 2013). This would suggest some removal of energy from the heterologous pathway, in order for the cell metabolism to deal with the stress from *p*-coumaric acid. The accumulation of *p*-coumaric acid may be due to a limited supply of acetyl-CoA needed for the formation of malonyl-CoA; thus, limiting 4CL activity. This view is in agreement with previous studies showing that supplied *p*-coumaric acid was only efficiently converted into naringenin after optimization of the malonyl-CoA supply (Xu et al., 2011; Kim et al., 2013).

A key step in the biosynthetic pathway of fisetin from L-tyrosine is the coordinated activities of CHR and CHS. These enzymes catalyze the conversion of *p*-coumaroyl-CoA into isoliquiritigenin and thus directing the metabolic flux in the biosynthetic pathway away from naringenin chalcone and subsequently naringenin, dihydrokaempferol, kaempferol and quercetin (Ballance and Dixon, 1995).

Two different approaches were evaluated to test the capability of CHR on directing the flux in the pathway towards isoliquiritigenin and subsequently liquiritigenin, garbanzol, resokaempferol and fisetin. (1) CHR from *A. mongholicus* was cloned downstream of its own T7 promoter on a high copy number plasmid and (2) CHR from *A. mongholicus* was fused together with CHS from *P. hybrida* on a medium copy number plasmid. The latter was carried out based on the idea that CHS and CHR perform protein-protein interactions (Winkel-Shirley, 1999).

Interestingly, the flux towards liquiritigenin was increased compared to naringenin when CHR was fused together with CHS, with concentration of liquiritigenin 18-fold higher than naringenin. In contrast, when CHR was cloned alone, the amount of liquiritigenin was only two-fold higher than naringenin. Thus

more flux was directed towards liquiritigenin, when CHR was fused together with CHS. Previously, by utilization of an *in vitro* enzymatic assay it was shown that purified CHR and CHS added in a 2:1 ratio, had a production ratio of 1:1 of liquiritigenin and naringenin (Welle and Schroder, 1992). This would suggest an overexpression of CHR compared to CHS could increase the flux towards liquiritigenin. However, we show that co-expression of CHS and CHR 1:1 (rather than separately) results in increased *in vivo* flux towards liquiritigenin in *E. coli*. In the subsequent part of the proposed pathway from liquiritigenin to resokaempferol through garbanzol, the enzymes F3H and FLS were evaluated for their ability to convert these compounds.

Indeed, the enzymes were shown to convert liquiritigenin into garbanzol and resokaempferol. Thus, FLS and F3H from *A. thaliana* are not only capable of catalyzing naringenin into kaempferol via dihydrokaempferol but also capable of catalyzing the conversion of liquiritigenin into garbanzol and subsequently resokaempferol (Fig. 1). This would suggest that these two enzymes from *A. thaliana* are promiscuous towards flavanones and that they have the ability to convert various flavanones into flavonols.

The major bottleneck in the generation of hydroxylated flavonoids in *E. coli*, such as the flavonols fisetin and quercetin, is the functional expression of the membrane associated plant P450 hydroxylases flavonoid 3′-hydroxylase (F3′H) and flavonoid 3′5′-hydroxylase (F3′5′H), due to the insolubility of these enzymes (Oeda et al., 1985), limitations of heme biosynthesis (Gallagher et al., 1992; Sinha and Ferguson, 1998), or lack of CPR function (Nelson et al., 1993; Porter et al., 1987). In order to achieve the biochemical synthesis of the hydroxylated flavonol fisetin from resokaempferol, we progressed with the functional expression of different flavonoid 3′-hydroxylase (F3′H) of different origins and reconstructed a previously reported flavonoid 3′-5′–hydroxylase (F3′5′H) from *C. roseus*, since the latter was shown to convert kaempferol into quercetin (Leonard et al., 2006). Furthermore, to ensure that only the hydroxylation of the 3′ position of the C ring of resokaempferol was targeted thereby enabling the conversion to fisetin, we primarily focused on F3′H enzymes. F3′5′H were excluded since they have previously been shown to perform both 3′ and 3′,5′ –hydroxylation reactions (Kaltenbach et al., 1999).

Using F3′H from *A. thaliana*, *F. x ananassa*, *M. x domestica* and *P. hybrida* we were able to convert resokaempferol into fisetin. Interestingly, even with protein sequences differing substantially from each other (similarity ranging from 48% to 97%), all P450's monooxygenase's investigated, demonstrated bioconversion abilities in converting resokaempferol into fisetin in the *E. coli* host.

The production of fisetin was considerably higher when F3′H from *A. thaliana* and *P. hybrida* were used to catalyze the step from resokaempferol to fisetin, compared to the remaining F3′H proteins evaluated here. Whether or not, this is due to a higher specificity, affinity, gene expression or overall function in *E. coli* remains to be investigated.

E. coli was chosen as a production host due to fast growth combined with easy handling and a vast set of molecular tools available. However, for the expression of plant cytochrome P450's the yeast *Saccharomyces cerevisiae* is usually the preferred host based on a superior protein expression machinery compared to *E. coli* (Zhou et al., 2015). Hence, *S. cerevisiae* is another attractive host for production of fisetin and related polyphenols.

The observed instability of fisetin and quercetin in the bacterial media can be potentially solved by glycosylation of the compounds, which in turn would stabilize them. Hence, a promising metabolic engineering strategy is the additional expression of a fisetin specific O-glycosyltransferase to the assembled pathway to produce fisetin glucoside and thereby to avoid fisetin degradation.

Finally, in order to evaluate the complete hypothetical pathway in a single cell of *E. coli,* the enzymes TAL, 4CL, CHSCHR, CHI, F3H,

FLS and F3′HCPR were expressed in *E. coli* and L-tyrosine used as a substrate for synthesis of fisetin. We show here for the first time an *E. coli* cell factory capable of converting the aromatic amino acid into fisetin. Except for *p*-coumaric acid and garbanzol no other intermediate could be detected, suggesting a full conversion of all intermediates and/or a low flux through the pathway.

This study elucidates and demonstrates a functional expression of a novel biosynthetic pathway towards the biosynthesis of the high-value plant compound fisetin in *E. coli*. Demonstrating the functionality of the different reported enzymatic steps to convert (I) L-tyrosine into liquiritigenin, (II) liquiritigenin into resokaempferol, (III) resokaempferol into fisetin and (IV) L- tyrosine into fisetin.

Finally, in order to further improve the created fisetin producing bacterial cell factory, described here, further pathway optimization could be conducted. This could be carried out using biosensors like the one recently published by Siedler et al. (2014), as well as cofactor engineering and increasing the supply of important precursors including malonyl-CoA.

Acknowledgments

Appendix A. Supporting information

Supplementary data associated with this article can be found in the online version at http://dx.doi.org/10.1016/j.ymben.2015.07.002.

References

Ballance, G.M., Dixon, R.A., 1995. *Medicago sativa* cDNAs encoding chalcone reductase. Plant Physiol. 107, 1027–1028.

Chemler, J.A., Yan, Y., Koffas, M.A., 2006. Biosynthesis of isoprenoids, polyunsaturated fatty acids and flavonoids in *Saccharomyces cerevisiae*. Microb. Cell Fact. 5, 20.

Cho, N., Choi, J.H., Yang, H., Jeong, E.J., Lee, K.Y., Kim, Y.C., Sung, S.H., 2012. Neuroprotective and anti-inflammatory effects of flavonoids isolated from Rhus verniciflua in neuronal HT22 and microglial BV2 cell lines. Food Chem. Toxicol. 50, 1940–1945.

Clere, N., Faure, S., Martinez, M.C., Andriantsitohaina, R., 2011. Anticancer properties of flavonoids: roles in various stages of carcinogenesis. Cardiovasc. Hematol. Agents Med. Chem. 9, 62–77.

Currais, A., Prior, M., Dargusch, R., Armando, A., Ehren, J., Schubert, D., Quehenberger, O., Maher, P., 2013. Modulation of p25 and inflammatory pathways by fisetin maintains cognitive function in Alzheimer's disease transgenic mice. Aging Cell..

Gallagher, J., Kaderbhai, N., Kaderbhai, M.A., 1992. Gene-dose-dependent expression of soluble mammalian cytochrome b5 in *Escherichia coli*. Appl. Microbiol. Biotechnol. 38, 77–83.

Gresele, P., Cerletti, C., Guglielmini, G., Pignatelli, P., de Gaetano, G., Violi, F., 2011. Effects of resveratrol and other wine polyphenols on vascular function: an update. J. Nutr. Biochem. 22, 201–211.

Hotze, M., Schroder, G., Schroder, J., 1995. Cinnamate 4-hydroxylase from *Catharanthus roseus*, and a strategy for the functional expression of plant cytochrome P450 proteins as translational fusions with P450 reductase in *Escherichia coli*. FEBS Lett. 374, 345–350.

Hwang, E.I., Kaneko, M., Ohnishi, Y., Horinouchi, S., 2003. Production of plant-specific flavanones by *Escherichia coli* containing an artificial gene cluster. Appl. Environ. Microbiol. 69, 2699–2706.

Kaltenbach, M., Schroder, G., Schmelzer, E., Lutz, V., Schroder, J., 1999. Flavonoid hydroxylase from *Catharanthus roseus*: cDNA, heterologous expression, enzyme properties and cell-type specific expression in plants. Plant J. 19, 183–193.

Kang, S.Y., Kang, J.Y., Oh, M.J., 2012. Antiviral activities of flavonoids isolated from the bark of *Rhus verniciflua* stokes against fish pathogenic viruses *in vitro*. J. Microbiol. 50, 293–300.

Katsuyama, Y., Matsuzawa, M., Funa, N., Horinouchi, S., 2008. Production of curcuminoids by *Escherichia coli* carrying an artificial biosynthesis pathway. Microbiology 154, 2620–2628.

Katz, M., Durhuus, T., Smits, H.P., Förster, J., 2011. Production of Metabolites. Patent no. WO2011147818.

Keasling, J.D., 2010. Manufacturing molecules through metabolic engineering. Science 330, 1355–1358.

Khan, N., Afaq, F., Khusro, F.H., Mustafa Adhami, V., Suh, Y., Mukhtar, H., 2012. Dual inhibition of phosphatidylinositol 3-kinase/Akt and mammalian target of rapamycin signaling in human nonsmall cell lung cancer cells by a dietary flavonoid fisetin. Int. J. Cancer 130, 1695–1705.

Kim, M.J., Kim, B.G., Ahn, J.H., 2013. Biosynthesis of bioactive O-methylated flavonoids in *Escherichia coli*. Appl. Microbiol. Biotechnol. 97, 7195–7204.

Kim, S.C., Kang, S.H., Jeong, S.J., Kim, S.H., Ko, H.S., Kim, S.H., 2012. Inhibition of c-Jun N-terminal kinase and nuclear factor kappa B pathways mediates fisetin-exerted anti-inflammatory activity in lipopolysccharide-treated RAW264.7 cells. Immunopharmacol. Immunotoxicol. 34, 645–650.

Leonard, E., Koffas, M.A., 2007. Engineering of artificial plant cytochrome P450 enzymes for synthesis of isoflavones by *Escherichia coli*. Appl. Environ. Microbiol. 73, 7246–7251.

Leonard, E., Yan, Y., Koffas, M.A., 2006. Functional expression of a P450 flavonoid hydroxylase for the biosynthesis of plant-specific hydroxylated flavonols in *Escherichia coli*. Metab. Eng. 8, 172–181.

Licandro-Seraut, H., Roussel, C., Perpetuini, G., Gervais, P., Cavin, J.F., 2013. Sensitivity to vinyl phenol derivatives produced by phenolic acid decarboxylase activity in *Escherichia coli* and several food-borne gram-negative species. Appl. Microbiol. Biotechnol. 97, 7853–7864.

Maher, P., 2009. Modulation of multiple pathways involved in the maintenance of neuronal function during aging by fisetin. Genes Nutr. 4, 297–307.

Maher, P., Akaishi, T., Abe, K., 2006. Flavonoid fisetin promotes ERK-dependent long-term potentiation and enhances memory. Proc. Natl. Acad. Sci. U. S. A. 103, 16568–16573.

Maher, P., Dargusch, R., Ehren, J.L., Okada, S., Sharma, K., Schubert, D., 2011. Fisetin lowers methylglyoxal dependent protein glycation and limits the complications of diabetes. PLoS One 6, e21226.

Malla, S., Koffas, M.A., Kazlauskas, R.J., Kim, B.G., 2012. Production of 7-O-methyl aromadendrin, a medicinally valuable flavonoid, in *Escherichia coli*. Appl. Environ. Microbiol. 78, 684–694.

Malla, S., Pandey, R.P., Kim, B.G., Sohng, J.K., 2013. Regiospecific modifications of naringenin for astragalin production in *Escherichia coli*. Biotechnol. Bioeng. 110, 2525–2535.

Matkowski, A., 2008. Plant *in vitro* culture for the production of antioxidants – a review. Biotechnol. Adv. 26, 548–560.

Middleton Jr, E., Kandaswami, C., Theoharides, T.C., 2000. The effects of plant flavonoids on mammalian cells: implications for inflammation, heart disease, and cancer. Pharmacol. Rev. 52, 673–751.

Nelson, D.R., Kamataki, T., Waxman, D.J., Guengerich, F.P., Estabrook, R.W., Feyereisen, R., Gonzalez, F.J., Coon, M.J., Gunsalus, I.C., Gotoh, O., 1993. The P450 superfamily: update on new sequences, gene mapping, accession numbers, early trivial names of enzymes, and nomenclature. DNA Cell Biol. 12, 1–51.

Oeda, K., Sakaki, T., Ohkawa, H., 1985. Expression of rat liver cytochrome P-450MC cDNA in *Saccharomyces cerevisiae*. DNA 4, 203–210.

Pan, M.H., Lai, C.S., Ho, C.T., 2010. Anti-inflammatory activity of natural dietary flavonoids. Food Funct. 1, 15–31.

Paterson, I., Anderson, E.A., 2005. Chemistry. The renaissance of natural products as drug candidates. Science 310, 451–453.

Porter, T.D., Wilson, T.E., Kasper, C.B., 1987. Expression of a functional 78,000 Da mammalian flavoprotein, NADPH-cytochrome P-450 oxidoreductase, in *Escherichia coli*. Arch. Biochem. Biophys. 254, 353–367.

Ross, J.A., Kasum, C.M., 2002. Dietary flavonoids: bioavailability, metabolic effects, and safety. Annu. Rev. Nutr. 22, 19–34.

Sagara, Y., Vanhnasy, J., Maher, P., 2004. Induction of PC12 cell differentiation by flavonoids is dependent upon extracellular signal-regulated kinase activation. J. Neurochem. 90, 1144–1155.

Sambrook, J., Fritsch, E., Maniatis, T., 1989. Molecular Cloning: A Laboratory Manual, 2nd ed. Cold Spring Harbor Laboratory Press, Cold Spring Harbor, NY.

Siedler, S., Stahlhut, S.G., Malla, S., Maury, J., Neves, A.R., 2014. Novel biosensors based on flavonoid-responsive transcriptional regulators introduced into *Escherichia coli*. Metab. Eng. 21, 2–8.

Simmler, C., Hajirahimkhan, A., Lankin, D.C., Bolton, J.L., Jones, T., Soejarto, D.D., Chen, S.N., Pauli, G.F., 2013. Dynamic residual complexity of the isoliquiritigenin–liquiritigenin interconversion during bioassay. J. Agric. Food Chem. 61, 2146–2157.

Sinha, N., Ferguson, S.J., 1998. An *Escherichia coli* ccm (cytochrome c maturation) deletion strain substantially expresses *Hydrogenobacter thermophilus* cytochrome c552 in the cytoplasm: availability of haem influences cytochrome c552 maturation. FEMS Microbiol. Lett. 161, 1–6.

Thill, J., Miosic, S., Gotame, T.P., Mikulic-Petkovsek, M., Gosch, C., Veberic, R., Preuss, A., Schwab, W., Stampar, F., Stich, K., Halbwirth, H., 2013. Differential expression of flavonoid 3′-hydroxylase during fruit development establishes the different B-ring hydroxylation patterns of flavonoids in *Fragaria x ananassa* and *Fragaria vesca*. Plant Physiol. Biochem. 72, 72–78.

Welle, R., Schroder, J., 1992. Expression cloning in *Escherichia coli* and preparative isolation of the reductase coacting with chalcone synthase during the key step in the biosynthesis of *soybean phytoalexins*. Arch. Biochem. Biophys. 293, 377–381.

Winkel-Shirley, B., 1999. Evidence for enzyme complexes in the phenylpropanoid and flavonoid pathways. Physiol. Plant. 107, 142–149.

Winkel-Shirley, B., 2001. Flavonoid biosynthesis. A colorful model for genetics, biochemistry, cell biology, and biotechnology. Plant Physiol. 126, 485–493.

Wu, J., Du, G., Zhou, J., Chen, J., 2013. Metabolic engineering of *Escherichia coli* for (2S)-pinocembrin production from glucose by a modular metabolic strategy. Metab. Eng. 16, 48–55.

Xu, P., Ranganathan, S., Fowler, Z.L., Maranas, C.D., Koffas, M.A., 2011. Genome-scale metabolic network modeling results in minimal interventions that cooperatively force carbon flux towards malonyl-CoA. Metab. Eng. 13, 578–587.

Xu, R.Y., Nan, P., Pan, H., Zhou, T., Chen, J., 2012. Molecular cloning, characterization and expression of a chalcone reductase gene from *Astragalus membranaceus Bge. var. mongholicus* (*Bge.*) Hsiao. Mol. Biol. Rep. 39, 2275–2283.

Yan, Y., Kohli, A., Koffas, M.A., 2005. Biosynthesis of natural flavanones in *Saccharomyces cerevisiae*. Appl. Environ. Microbiol. 71, 5610–5613.

Yan, Y., Huang, L., Koffas, M.A., 2007. Biosynthesis of 5-deoxyflavanones in microorganisms. Biotechnol. J. 2, 1250–1262.

Ying, T.H., Yang, S.F., Tsai, S.J., Hsieh, S.C., Huang, Y.C., Bau, D.T., Hsieh, Y.H., 2012. Fisetin induces apoptosis in human cervical cancer HeLa cells through ERK1/2-mediated activation of caspase-8-/caspase-3-dependent pathway. Arch. Toxicol. 86, 263–273.

Zandi, K., Teoh, B.T., Sam, S.S., Wong, P.F., Mustafa, M.R., Abubakar, S., 2011. Antiviral activity of four types of bioflavonoid against dengue virus type-2. Virol. J. 8 (560–422X-8-560).

Zhou, K., Qiao, K., Edgar, S., Stephanopoulos, G., 2015. Distributing a metabolic pathway among a microbial consortium enhances production of natural products. Nat. Biotechnol. 33, 377–383.